Chimia 55 (2001) 1053–1057

ISSN 0009–4293

NMR Spectroscopy: Increased Sensitivity for Detecting Heteronuclear ^{1}H-^{13}C Couplings through Multiple and Single Bonds

Rémy Burger[a], Christian Schorn[b], and Peter Bigler[a]*

Abstract: A new 2D pulse sequence HMSC (**H**eteronuclear **M**ultiple- and **S**ingle-bond coupling **C**orrelations) for the simultaneous detection of long-range and one-bond heteronuclear connectivities is proposed, which allows the two types of responses to be separated and the corresponding $^{n}J_{CH}$ and $^{1}J_{CH}$ connectivity maps to be calculated. Unlike standard methods, designed to measure one single type of heteronuclear spin–spin interaction, and to efficiently suppress the other, both $^{n}J_{CH}$ and $^{1}J_{CH}$ are measured simultaneously in a single experiment with the HMSC pulse sequence. Compared to the common strategy with two standard experiments applied one after the other, *e.g.* HMBC and HMQC, valuable measuring time may be saved with this single experiment approach. The efficiency of the new pulse sequence and the quality of the corresponding spectra is demonstrated and compared with the results obtained with the standard HMBC experiment using bacdanol.

The attractive and unique single experiment approach together with its easy experimental set-up and straightforward data processing makes HMSC a valuable experimental alternative for the today's more time-consuming 'two-step' practice and makes it suitable for standard routine applications.

Keywords: HMBC · HMQC · HMSC · Long-range heteronuclear shift correlation · One-bond heteronuclear shift correlation

1. Introduction

High-resolution NMR has developed into the most powerful analytical tool for the elucidation of molecular structures. Structural information obtained from a variety of dedicated experiments and the analysis of the corresponding spectra allows functional groups to be recognized, structural fragments to be connected and the detailed 3D structure of molecules, including their dynamic properties, to be established in a highly reliable manner.

*Correspondence: Prof. P. Bigler[a]
[a]Department of Chemistry and Biochemistry
University of Bern
Freiestrasse 3
CH-3012 Bern
Tel.: +41 31 631 39 48
Fax: +41 31 631 34 24
E-Mail: bigler@ioc.unibe.ch
http://www.nmr.unibe.ch/
[b]Institute of Molecular Biology
ETH Hönggerberg
CH-8093 Zürich

Despite its popularity, NMR suffers from inherent low detection sensitivity caused by the relatively small energy differences between the different magnetic states of atomic nuclei and the low natural abundance of the magnetic active isotope for heteronuclei such as ^{13}C or ^{15}N.

Efforts to overcome this problem have been undertaken on different levels: Taking advantage of new hardware technologies spectrometer magnets with field strengths of up to 21 Tesla (900 MHz ^{1}H resonance frequency) and superconducting probeheads ('cryo-probes'), both probably most effective for improving the detection sensitivity, have been built and introduced. Various sophisticated techniques for isotopic enrichment ('isotopic labeling') have been developed and are now widely used for the NMR spectroscopic investigation of biomolecules. Modern pulse sequences taking advantage of sensitivity-enhancing options such as ^{1}H detection ('inverse experiments') or principles such as the recently introduced TROSY technique for the investigation of biomolecules with molecular sizes beyond 100 kDa have been designed. Last but not least optimized data processing exploiting signal-to-noise enhancement by linear prediction or maximum entropy techniques may be used for final spectral improvements.

In this contribution we would like to focus on a further possibility for improving the overall sensitivity of NMR experiments, which is based on the following. More demanding structural problems are most efficiently and unequivocally solved following a 'multi-parameter approach', thereby taking advantage of various structure-dependent NMR parameters. For solving a given structural problem, the most suitable and adequate parameters such as indirect homo- and heteronuclear spin–spin coupling connectivities, the corresponding coupling constants and signal multiplicities, direct spin–spin coupling connectivities and corresponding NOEs and parameters for characterizing the dynamic properties of molecules are evaluated. Depending on the com-

plexity of the structural problem and since most of today's NMR experiments are dedicated to detecting only one of these parameters at a time, a series of experiments has to be performed one after the other. This may become rather time-consuming in the case of small sample amounts and/or with more demanding less sensitive experiments.

Experiments designed for the simultaneous detection of different types of parameters, *e.g.* heteronuclear long-range and one-bond spin–spin connectivities, in a single rather than separate experiments and allowing the different types of parameters to be disentangled and to be displayed in different spectra would be appreciated. Assuming equal or similar sensitivities compared to the corresponding 'single parameter' standard experiments valuable spectrometer time could be economized.

Very recently such a 'combined' 2D experiment for the simultaneous detection of **H**eteronuclear **M**ultiple and **S**ingle-bond **C**orrelations HMSC [1] has been developed in our group. Whereas one-bond ($^1J_{CH}$) connectivities and coupling constants are mainly used to check and establish signal assignments of proton-bearing carbons and to extract information on functional groups and carbon hybridization respectively, multiple-bond ($^nJ_{CH}$) connectivities and coupling constants are probably much more valuable for establishing molecular structures. 'Long-range' connectivities allow signal assignments, including quaternary carbons, to be completed and structural fragments to be connected unequivocally. Corresponding coupling constants allow complex stereochemical problems to be solved in a straightforward way. Reliable ^{13}C signal assignments based on $^1J_{CH}$ connectivities and assigned ^1H signals are a prerequisite, however, for the interpretation of $^nJ_{CH}$ correlation spectra. Consequently, information on both types of coupling interactions is usually needed for unequivocal conclusions with more demanding structural problems.

In this contribution the application of the HMSC experiment to bacdanol is demonstrated.

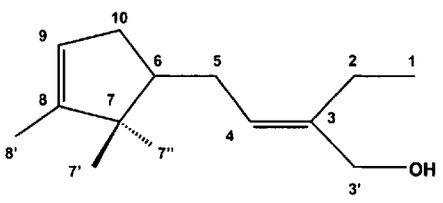

2. Results and Discussion

The starting point for our efforts in pulse sequence design was the prominent HMBC [2] experiment and its modern variants [3] for selectively detecting heteronuclear long-range couplings. Despite its high detection sensitivity, the gradient enhanced HMBC experiment suffers from a poor low-pass filter quality with breakthrough of unwanted $^1J_{CH}$ signals. Furthermore, the experiment may not be adjusted to sample the wide range of $^nJ_{CH}$ coupling constants (1–25 Hz) in a uniform manner and important cross peaks may be rather weak or may even be lost in a HMBC spectrum.

Modified variants to improve low-pass filter efficiency with the implementation of an additional BIRD-relaxation filter [4], an additional TANGO filter [5], and a BIRD-J filter [6] have been developed. Efforts for uniform sampling of long-range couplings have been undertaken and corresponding experiments have been proposed, *e.g.* a 3D HMBC [7] with the third dimension used for 'scanning' the whole range of $^nJ_{CH}$ couplings. Among these developments the ACCORDION-HMBC [8], the IMPEACH-HMBC [9], and the CIGAR-HMBC [10] experiments are probably the most popular and promising since they not only suppress $^1J_{CH}$ signals more efficiently, but sample in a systematic fashion and in a single experiment a potentially wide range of long-range couplings exploiting the ACCORDION principle [11]. They are designed as 'refocused' variants for optional ^{13}C broadband decoupling during data acquisition. However, a few minor drawbacks remain with these experiments with a general loss of sensitivity compared to the basic HMBC as the most severe problem. Therefore the main requirements for a more efficient 'combined' alternative may be summarized as follows: Simultaneous detection of $^nJ_{CH}$ and $^1J_{CH}$ connectivities; equal or at least similar sensitivities especially for measuring $^nJ_{CH}$ connectivities compared to today's state-of-the-art experimental alternatives; powerful filters for rejecting unwanted $^1J_{CH}$ signals in the final $^nJ_{CH}$ subspectrum ('$^nJ_{CH}$ low-pass' filter) and *vice-versa* for rejecting unwanted $^nJ_{CH}$ signals in the final $^1J_{CH}$ subspectrum ('$^1J_{CH}$ high-pass' filter); unlimited applicability with respect to the range of $^nJ_{CH}$ and $^1J_{CH}$ coupling constants, the corresponding multiplicities and the degree of complexity in the ^1H spectrum; easy experimental set-up for routine applications.

As a result Fig. 1 shows the correspondingly developed HMSC experiment.

The HMSC experiment starts with a 90° ^1H pulse, followed by a $BIRD_y$ element [12], incorporated in the middle of the delay for the evolution of long-range coupling interactions. The corresponding delays $D2 = (2 \cdot {}^1J_{CH})^{-1}$ and $D3 = (4 \cdot {}^nJ_{CH})^{-1}$ are adjusted for one-bond and long-range couplings respectively. Neglecting homonuclear couplings, longitudinal z-magnetization of one-bond and long-range coupled protons (^1I_z, ^nI_z) is transformed into transverse magnetization by the initial 90° ^1H pulse (^1I_z, $^nI_z \rightarrow -{}^1I_y$, $-{}^nI_y$). Transverse magnetization evolves in the course of the $BIRD_y$ element either and exclusively under the influence of long-range couplings for $^nJ_{CH}$ coupled protons ($-{}^nI_y \rightarrow 2^nI_xS_z$), or under the influence of ^1H chemical shifts for $^1J_{CH}$ coupled protons ($-{}^1I_y \rightarrow -{}^1I_y$, ^1I_x) as described in detail elsewhere [12]. This allows coherence of $^nJ_{CH}$ coupled protons to be labeled selectively at this stage of the pulse sequence with a ^{13}C pulse adjusted either to 180° or 0° ($2^nI_xS_z \rightarrow \pm 2^nI_xS_z$), whereas coherence of $^1J_{CH}$ coupled protons is not affected by the ^{13}C pulse ($-{}^1I_y$, $^1I_x \rightarrow -{}^1I_y$, ^1I_x). In contrast to the in-phase $^1J_{CH}$ coherence, which evolves under the influence of one-bond couplings and proton chemical shifts into antiphase coherence ($-{}^1I_y$, $^1I_x \rightarrow 2^1I_xS_z$, $2^1I_yS_z$) in the subsequent D2 delay, almost no additional coupling evolution occurs for $^nJ_{CH}$ coherence. The next 90° ^{13}C pulse transforms $^nJ_{CH}$ and $^1J_{CH}$ antiphase components into multiquantum coherences, which evolve in t1 exclusively under the influence of ^{13}C chemical shifts. $^nJ_{CH}$ and $^1J_{CH}$ multiquantum coherences are transformed back into detectable proton single-quantum coherences by the last 90° ^{13}C pulse and are detected simultaneously with no ^{13}C broadband decoupling during data acquisition.

To preserve and exploit the $^nJ_{CH}$ selective labeling of proton signals, achieved with the composite ^{13}C pulse for the subsequent separation of one-bond and 'long-range' responses in two subspectra, FIDs are acquired in the so-called 'interleaved mode'. For each t1 increment, two FIDs with the phase of the first ^{13}C 180° pulse set as y or -x respectively (Fig. 1) are acquired and stored separately. In a first step of data processing, each t1 pair is split and two intermediate 2D matrices are generated from the original 2D data matrix. To obtain the final two spectra with the $^1J_{CH}$ and $^nJ_{CH}$ responses disentangled from each other,

CHIMIA 2001, 55, No. 12

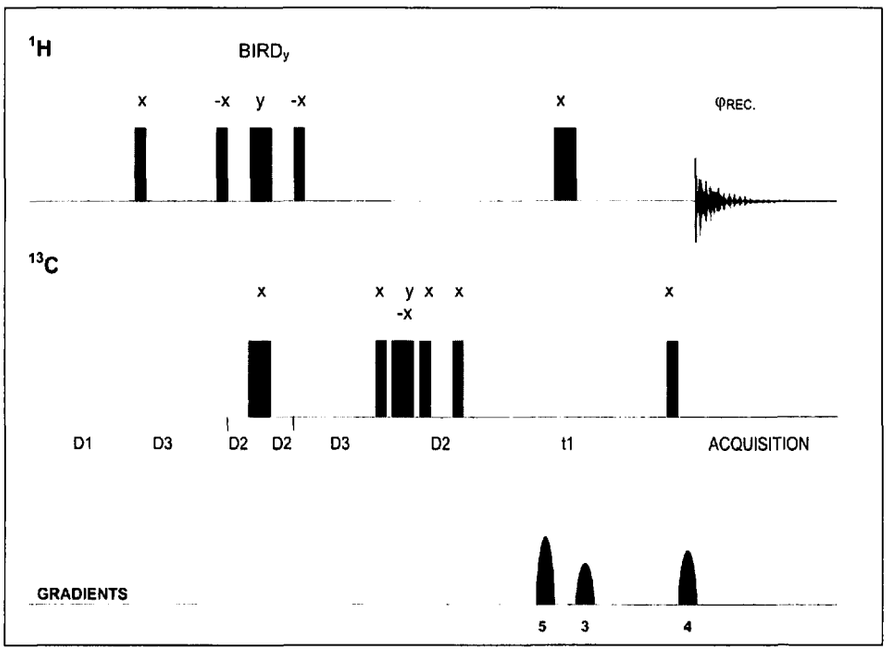

Fig. 1. HMSC pulse sequence for the detection of $^nJ_{CH}$ and $^1J_{CH}$ connectivities. Thin and thick bars represent 90° and 180° pulses, respectively. The first 180° ^{13}C pulse is replaced by a $90°_x$–$180°_y$–$90°_x$ composite pulse. D2 is set to $(2\cdot{}^1J_{CH})^{-1}$ and D3 is set to $(4\cdot{}^nJ_{CH})^{-1}$. For each t1 value two t2-FIDs with different phase settings for the second 180° ^{13}C pulse (y, –x) are acquired and separately stored ('interleaved' mode of detection). The full phase cycle is given in [1]. Using standard BRUKER software the two t1 sets differing in the sign of $^nJ_{CH}$ proton signals are disentangled and stored in two submatrices, which are either added to or subtracted from each other to calculate the final data matrices with the $^1J_{CH}$ and $^nJ_{CH}$ responses separated (spectral editing). The BRUKER DRX pulse program and the modified BRUKER SPLITSER.AU programs for data processing (see Fig. 2) are available from the authors upon request.

these two intermediate 2D matrices are added to, and subtracted from each other respectively (spectral editing). Data are processed in the same way as the HMBC data and the corresponding 2D magnitude mode (in F1) spectra are then calculated (for details see captions of Fig. 2 and Fig. 3).

For measuring ^{13}C broadband decoupled spectra, $^nJ_{CH}$ and $^1J_{CH}$ coherences have to be refocused prior to data acquisition. This may be accomplished with two additional BIRD elements ($BIRD_y$ and $BIRD_x$) after the t1 period and with the phase cycle and gradient pulse settings adjusted accordingly.

The HMSC sequence was applied to bacdanol. For comparison, spectra were acquired with the basic HMBC and HMQC experiments. In order to compare the results, experimental conditions were set as similar as possible and exactly the same measuring times were maintained with each experiment. Consequently, either the $^1J_{CH}$ or the $^nJ_{CH}$ spectrum could be acquired within this pre-set measuring time with the HMQC and the HMBC experiments respectively, whereas both types of spectra could be obtained with the HMSC experiment and adequate data processing.

Fig. 2 shows expansions (aliphatic part) of the $^nJ_{CH}$ (left) and the $^1J_{CH}$ (right) connectivity spectra of bacdanol obtained with the HMSC experiment. The excellent discrimination between $^nJ_{CH}$ and $^1J_{CH}$ cross peaks is obvious in the two sub-spectra of the HMSC experiment. Each spectrum contains one type of cross peaks – $^nJ_{CH}$ and $^1J_{CH}$ respectively – only.

Fig. 3 shows representative rows (responses of C(3') and C(10)) measured with the HMSC and the standard gradient enhanced HMBC experiment respectively. For carbon C(3') intense long-range $^3J_{CH}$ connectivities to H-C(2) and H-C(4) are measured. The row for carbon C(10) on the other hand shows $^2J_{CH}$ connectivities to H-C(6) and H-C(9), $^3J_{CH}$ connectivities to the two non-equivalent H(5) protons and weak $^4J_{CH}$ connectivity to the methyl protons H-C(8'). All these heteronuclear long-range connectivities are in full agreement with the expectations for the given structure.

Concentrating on sensitivity first, it follows from Fig. 3, that with the HMSC experiment, only minor sensitivity losses have to be taken into account for detecting long-range interactions compared to the HMBC experiment. For one-bond interactions, as simultaneously obtained with the HMSC experiment, a decrease in sensitivity of about 15% compared to the non-decoupled HMQC spectrum (not shown) has been observed, most probably because of additional relaxation losses with the long D3 delays. A decrease in sensitivity of about 50% has to be taken into account compared to the ^{13}C GARP decoupled HMQC spectrum. Signal intensities are nevertheless well above the intensities of most of the $^nJ_{CH}$ cross peaks and their doublet structure may not severely complicate spectral analysis.

Concentrating on filter efficiencies next, excellent results are obtained for the more demanding $^nJ_{CH}$ spectra with the HMSC experiment. Extremely high $^1J_{CH}$ suppression degrees are of utmost importance and a prerequisite for the reliable detection and recognition of very weak

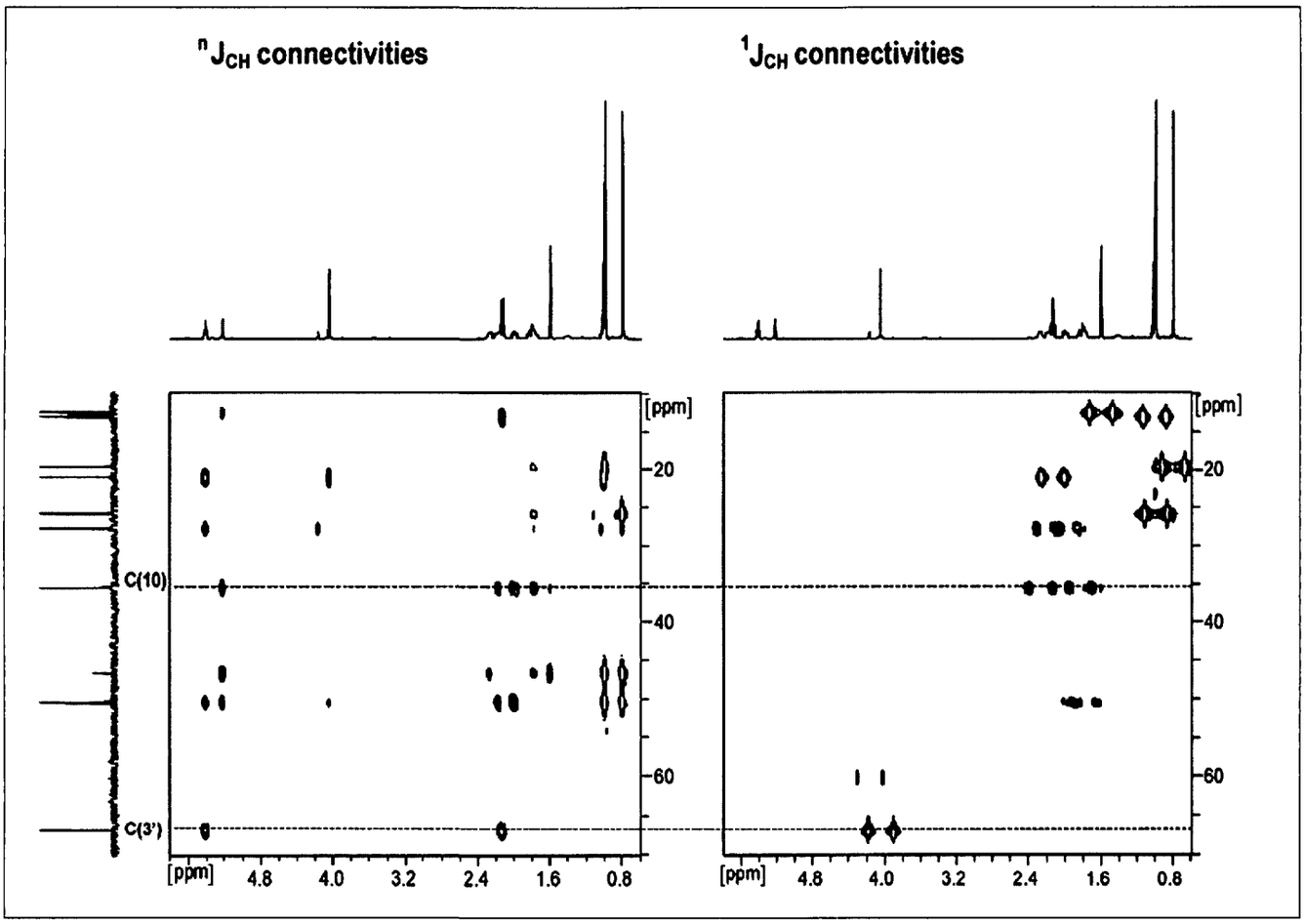

Fig. 2. $^{n}J_{CH}$ and $^{1}J_{CH}$ 2D spectra of bacdanol (expansion of the aliphatic region) measured with the HMSC pulse sequence. The experiments were performed on a Bruker DRX-500 spectrometer operating at a proton resonance frequency of 500.13 MHz with a 5 mm inverse probehead (TBI) equipped with additional coils for z-gradients and with 90° pulse lengths of 7.5 μs and 15 μs for ^{1}H and ^{13}C respectively. Delays D1, D2 ($2 \cdot {}^{1}J_{CH}^{-1}$) and D3 ($4 \cdot {}^{n}J_{CH}^{-1}$) were set as 2s, 3.45 ms (optimized for $^{1}J_{CH}$ = 145Hz) and 25 ms (optimized for $^{n}J_{CH}$ = 10 Hz) respectively. The delay for phase switching within the ^{13}C composite pulses was set to 5 μs.
Each 2D spectrum was collected with ^{1}H and ^{13}C spectral widths of 3094 Hz and 21379 Hz respectively. Eight scans using 2048 data points in t2 were acquired for each of 2 x 256 FIDs with 'interleaved' mode of detection. In a first step of data processing the original 2D data were split into two new data sets by using the slightly modified SPLITSER.AU (BRUKER) program. Each of these two data sets was apodized with a 45° shifted sine square function and Fourier transformed in t2. To disentangle the responses of one-bond and long-range coupling interactions, these data sets were then added to and subtracted from each other. The final $^{1}J_{CH}$ and $^{n}J_{CH}$ subspectra were obtained after apodization with a non-shifted sine square function, zero-filling to 512 points and Fourier transformation in t1 and with magnitude mode calculation in F1. The same contour levels are used for both subspectra. Rows for C(3') and C(10) are indicated.

long-range couplings valuable for the connecting remote molecular fragments. Such cross peaks may otherwise be overlooked, may be mistaken for or may be accidentally hidden by residual $^{1}J_{CH}$ peaks. Whereas the residual $^{1}J_{CH}$ peaks (denoted by an asterisk) visible in the rows extracted from the HMBC spectrum do not affect spectral interpretation for row C(3'), reliable recognition of long-range peaks for row C(10) with partial overlap of $^{1}J_{CH}$ and $^{n}J_{CH}$ peaks is no longer possible. The high $^{1}J_{CH}$ suppression degrees obtained with the HMSC experiment on the other hand allows the reliable recognition of even weak long-range interactions such as the $^{4}J_{CH}$ connectivity between C(10) and the methyl protons H-C(8').

Suppression of $^{n}J_{CH}$ cross peaks in HMSC $^{1}J_{CH}$ subspectra – although no such residual peaks are seen in rows C(3') and C(10) – is usually less efficient. However, '$^{1}J_{CH}$ high-pass' filtering is less demanding since one-bond cross peaks clearly dominate and their doublet structure may easily be recognized.

Improvements for the HMSC experiment such as the implementation of optimized phase cycles, the incorporation of broadband excitation over a range of long-range couplings, the study of alternative gradient settings allowing absorption profiles to be calculated in the F1 dimension and the critical comparison of the HMSC experiment with a recently proposed alternative 'dual experiment', the MBOB pulse sequence [13], are in progress.

3. Conclusion

Information on both long-range and one-bond coupling networks, deduced from correspondingly edited correlation spectra with highest discrimination factors are not only highly desirable for unequivocal signal assignments, but a prerequisite for the reliable solution of more demanding structural problems.

The HMBC-derived 2D HMSC pulse sequence for the efficient measurement of $^{n}J_{CH}$ and $^{1}J_{CH}$ connectivities takes advantage of a strategy which deviates considerably from usual strategies in pulse sequence design. Instead of destructively suppressing 'unwanted' $^{1}J_{CH}$ responses in the HMBC experiment by one or several filters, both types of coherences are

CHIMIA 2001, 55, No. 12

detected simultaneously in each scan and in such a way that $^{n}J_{CH}$ and $^{1}J_{CH}$ responses can be disentangled and corresponding connectivity maps can be calculated.

With similar sensitivities for detecting $^{n}J_{CH}$ interactions compared to the standard HMBC and despite a less attractive sensitivity for the detection of $^{1}J_{CH}$ interactions an overall gain in sensitivity results with the HMSC experiment compared to the usual strategy with two $^{1}J_{CH}$ and $^{n}J_{CH}$ dedicated experiments performed one after the other.

Features such as the outstanding suppression degree for $^{1}J_{CH}$ signals in the $^{n}J_{CH}$ spectra for the whole range of one-bond and long-range couplings, the insensitivity to incorrectly set ^{13}C pulse angles and the easy experimental set-up with simple data processing makes HMSC a valuable alternative to today's less-efficient two-experiment approach and suitable for routine applications.

Received: October 17, 2001

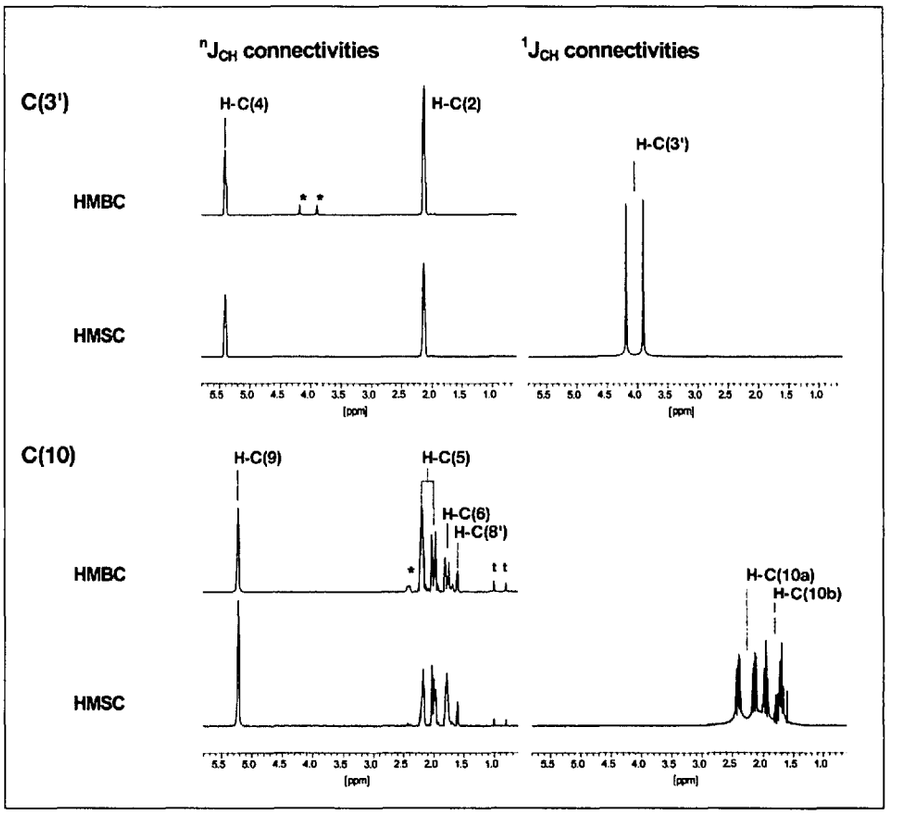

Fig. 3. Representative rows with the $^{n}J_{CH}$ and $^{1}J_{CH}$ connectivities of C(3') and C(10) demonstrating the sensitivities and lineshapes obtained with the HMBC and the HMSC experiment are shown. The same experimental parameters were used for the HMBC (with the long-range evolution delay adjusted for $^{n}J_{CH}$ = 10Hz) as given for the HMSC experiment (see Fig. 2). To take into account the additive/subtractive combination of two FIDs with HMSC data processing 16 (instead of 8) scans were acquired for each of the 256 FIDs with the HMBC experiment. For processing the HMBC data the same parameters for apodization, zero-filling and the FT mode were used as given for the HMSC experiment (see Fig. 2).^{1}H-signals of corresponding long-range cross peaks are assigned. Residual $^{1}J_{CH}$ signals and signals originating from t1-noise are indicated with an asterisk and a 't' respectively.

[1] R. Burger, C. Schorn, P. Bigler, *J. Magn. Reson.* **2001**, *148*, 88.

[2] A. Bax, M.F. Summers, *J. Am. Chem. Soc.* **1986**, *108*, 2093.

[3] a) W. Willker, D. Leibfritz, R. Kerssebaum, R. Bermel, *Magn. Reson. Chem.* **1993**, *31*, 287; b) S. Braun, H.-O. Kalinowski, S. Berger, '150 and More Basic NMR Experiments', Wiley-VCH, Weinheim **1998**; c) K. Furihata, H. Seto, *Tetrahedron Lett.* **1995**, *36*, 2817; d) R. Marek, L. Králík, V. Sklenár, *Tetrahedron Lett.* **1997**, *38*, 665; e) S. Sheng, H. van Halbeek, *J. Magn. Reson.* **1998**, *130*, 296; f) K. Furihata, H. Seto, *Tetrahedron Lett.* **1998**, *39*, 7337.

[4] G. Martin, A. Zektzer, in '2D NMR Methods for Establishing Molecular Connectivity', VCH, Weinheim, **1988**, 267.

[5] T. Parella, F. Sanchez-Ferrando, A. Virgili, *J. Magn. Reson.* **1995**, *112*, 241.

[6] R. Burger, C. Schorn, P. Bigler, *Magn. Reson. Chem.* **2000**, *38*, 963.

[7] K. Furihata, H. Seto, *Tetrahedron Lett.* **1996**, *37*, 8901.

[8] R. Wagner, S. Berger, *Magn. Reson. Chem.* **1998**, *36*, 44.

[9] C.E. Hadden, G.E. Martin, V.V. Krishnamurthy, *J. Magn. Reson.* **1999**, *140*, 274.

[10] C.E. Hadden, G.E. Martin, V.V. Krishnamurthy, *Magn. Reson. Chem.* **2000**, *38*, 143.

[11] G. Bodenhausen, R.R. Ernst, *J. Am. Chem. Soc.* **1982**, *104*, 1304.

[12] J.R. Garbow, D.P. Weitekamp, A. Pines, *Chem. Phys. Lett.* **1982**, *93*, 504.

[13] A. Meissner, O.W Sørensen, *Magn. Reson. Chem.* **2000**, *38*, 981.